

Accepted Manuscript

Assembly of Nitroreductase and Layered Double Hydroxides toward Functional Biohybrid Materials

Felipe Bruna, Christine Mousty, Pascale Besse-Hoggan, Isabelle Batisson, Vanessa Prevot

PII: S0021-9797(18)30889-0
DOI: <https://doi.org/10.1016/j.jcis.2018.07.126>
Reference: YJCIS 23917

To appear in: *Journal of Colloid and Interface Science*

Received Date: 24 April 2018
Revised Date: 24 July 2018
Accepted Date: 28 July 2018

Please cite this article as: F. Bruna, C. Mousty, P. Besse-Hoggan, I. Batisson, V. Prevot, Assembly of Nitroreductase and Layered Double Hydroxides toward Functional Biohybrid Materials, *Journal of Colloid and Interface Science* (2018), doi: <https://doi.org/10.1016/j.jcis.2018.07.126>

This is a PDF file of an unedited manuscript that has been accepted for publication. As a service to our customers we are providing this early version of the manuscript. The manuscript will undergo copyediting, typesetting, and review of the resulting proof before it is published in its final form. Please note that during the production process errors may be discovered which could affect the content, and all legal disclaimers that apply to the journal pertain.



Assembly of Nitroreductase and Layered Double Hydroxides toward Functional Biohybrid Materials

Felipe Bruna^{†‡}, Christine Mousty[†], Pascale Besse-Hoggan[†], Isabelle Batisson[‡], Vanessa Prevot^{†}*

[†]Université Clermont Auvergne, CNRS, Sigma-Clermont, ICCF, Institut de Chimie de Clermont-Ferrand, F-63000 CLERMONT-FERRAND, France

[‡]Université Clermont Auvergne, CNRS, Laboratoire Microorganismes : Génome et Environnement, F-63000 CLERMONT-FERRAND, France

KEYWORDS: enzyme immobilization, layered double hydroxides, nitroreductase, biohybrid materials, biomolecules, mesotrione

ABSTRACT

The development of new multifunctional materials integrating catalytically active and selective biomolecules, such as enzymes, as well as easily removable and robust inorganic supports that allow their use and reuse, is a subject of ongoing attention. In this work, the nitroreductase NfrA2/YncD (NR) from *Bacillus megaterium* Mes11 strain was successfully immobilized by adsorption and coprecipitation on layered double hydroxide (LDH) materials with different compositions (MgAl-LDH and ZnAl-LDH), particle sizes and morphologies, and using different enzyme/LDH mass ratios (Q). The materials were characterized and the immobilization and

catalytic performance of the biohybrids were studied and optimized. The nitroreductase-immobilized on the nanosized MgAl-LDH displayed the best catalytic performance with 42-46% of catalytic retention and more than 80% of immobilization yield at saturation values of enzyme loading $C_s \approx 0.6$ g NR/g LDH ($Q = 0.8$). The adsorption process displayed high enzyme-LDH affinity interactions yielding to a stable biohybrid material. The increase in the amount of enzyme loading favoured the catalytic performance of the biohybrid due to the better preservation of the native conformation. The biohybrid was reused several times with partial activity retention after 4 cycles. In addition, the biohybrid was successfully dried maintaining the catalytic activity for several weeks when it was stored in its dry form. Finally, thin films of NR@LDH biohybrid deposited on glassy carbon electrodes were evaluated as a modified electrode applied for nitro-compound detection. The results show that these biohybrids can be used in biotechnology applications to efficiently detect compounds such as dinitrotoluene. The search for new non-hazardous chemical designs preventing or reducing the use of aggressive chemical processes for human being and the environment is the common philosophy within sustainable chemistry.

1. INTRODUCTION

Highly reactive and selective microbial biomolecules, such as enzymes, are recognized as powerful tools involved in many well-established natural and synthetic processes. In the last decades, the enzyme immobilization has gained worldwide interest for a more widespread use ranging from industrial biotransformation, biosensing, drug delivery to food processing [1-4].

Indeed enzyme immobilization on suitable supports produces heterogeneous biohybrids with potentially new functionalities synergistically offered at molecular scale by the intrinsic properties of the host material and its interactions with biomolecules. The produced functional biohybrids usually display interesting advantages such as the possibility of reuse, improved

operational stability, ease of separation of the reaction medium, reduction of contamination in the final product and improvement in the control of biocatalytic reactions.

Obviously, both the immobilization process and the type of support are key factors for an optimal biohybrid performance. Several techniques for the enzyme immobilization were described in the literature, such as adsorption, entrapment, covalent binding or cross linking [5, 6]. With the aim of a cost-effectiveness biohybrid, the immobilization technique should be simple and inexpensive, using chemically soft and reproducible processes and avoiding hazardous solvents or reagents. Different types of organic and inorganic materials have been extensively studied and reported as efficient supports for enzyme immobilization, such as chitosan, cellulose, epoxide-containing polymers, silica, oxides and clays, evidencing the need of optimizing the conditions for each enzyme/immobilization matrix couple [5, 7-11].

Among the various supports available, layered double hydroxides (LDH) show many advantages compared to other organic and inorganic host structures, such as improved physico-chemical stability, biocompatibility and resistance to microbiological attacks. Within the potential inorganic supports, LDH are promising materials especially due to their large surface area with abundant basic binding sites, 2D open framework, unique exchange properties, tuneable particle size and low cost [12]. LDH, also referred as anionic clays, can be described according to a brucite-type metal hydroxide structure with a general formula $[M_{1-x}^{II}M_x^{III}(OH)_2]^{x+} X_{x/n}^{n-} \cdot mH_2O$. On one hand, the molar ratio and the type of divalent, M^{II} , and trivalent, M^{III} , metals in the layers control the physico-chemical properties like the charge density or basicity of the materials. On the other hand, the type and nature of the exchangeable anion, X^n , may modify their adsorption properties. These features provide to the LDH compounds a high structural and morphological versatility. Such kind of inorganic materials have been extensively studied as matrices of confinement for various biomolecules ranging from amino acids, DNA, to enzymes,

other proteins and even bacteria [13-16]. Indeed, several enzymes such as alkaline phosphatase, lipase, α -amylase or transketolase have been successfully immobilized and characterized on different phases of LDH-type materials through various immobilization strategies, evidencing the need of optimizing the process for each enzyme to access to efficient biohybrid [17-20]. Likewise, some applications involving enzymes/LDH biohybrids have been described in the literature, especially as biocatalysts or biosensors [21, 22].

Nitroreductases are interesting enzymes able to reduce nitroaromatic derivatives often highly toxic, mutagenic, or carcinogenic which makes them of great interest for potential environmental applications [23]. The reduction of nitroaromatic compounds is catalysed *via* a two or one-electron transfer by nitroreductase type I or II, respectively [24, 25]. Recently, we have identified and produced nitroreductases called NfrA1 and NfrA2/YcnD from *Bacillus megaterium* Mes 11 capable to biotransform mesotrione (See supporting information Figure S1), an herbicide belonging to the triketone family broadly used on maize crops and having a nitroaromatic moiety [26, 27]. These enzymes belong to the NfrA Frp family of the nitro-flavine mononucleotide (FMN) reductase superfamily (oxygen insensitive nitroreductase type I) using nicotinamide adenine dinucleotide phosphate (NADPH) or nicotinamide adenine dinucleotide (NADH) as cofactors [28]. Its broad activity spectrum for biotransforming several nitroaromatic compounds including insecticides, fungicides, antibiotics and prodrugs opens the way to various opportunities for potential applications of NfrA2/YcnD, for instance in biosensor development or bioremediation as suggested by Carles et al. [26].

It is noteworthy to mention that in the literature, there is little work that has the immobilization of enzymes with nitroreductase activity (See supporting information Table S1). A nitroreductase from *E. cloacae* fused with a maltose binding protein, and immobilized on glassy carbon electrodes (GCE) by entrapment within redox active organic polymer, was applied as biosensor

for the detection of 2,4,6-trinitrotoluene (TNT) [29]. Recently, Komarova et al. [30] reported a nitroreductase-modified ion-selective field effect transistor for the detection of TNT and other nitroaromatic explosives. Additionally, the immobilization of the nitrobenzene nitroreductase from *P. pseudoalcaligenes* JS45 on polyethyleneimine-mediated silica particles and the immobilization of a genetically modified nitroreductase from *E. coli* on gold nanoparticles have been described for the activation of the CB1954 cancer prodrug [31, 32].

In this work, we were interested to investigate the efficiency of LDH to immobilize nitroreductases which in our knowledge, has never been reported. Having in mind the elements exposed above, we report here a rational approach to the development and characterization of NfrA2/YcnD (NR) immobilized biohybrids using LDH compounds as supports. For that, Mg/Al and Zn/Al LDH matrices were prepared and characterized. The enzyme immobilization on those LDH phases was carried out using different soft chemical routes: adsorption or direct coprecipitation. Thus, the so-prepared biohybrids were characterized and the performance of the different NR@LDH biohybrids for the mesotrione-biotransformation was assayed. Additionally, the NR activity was also studied electrochemically to investigate the suitability of NR-based biohybrids for biotechnology applications, such as biosensors.

2. EXPERIMENTAL SECTION

2.1. Reagents

Bradford reagent was obtained from Bio-Rad and Ni-NTA resin from Qiagen. Bovine serum albumin (BSA, purity > 98%), mesotrione (Pestanal[®], purity 99.9%), 2,3 dinitrotoluene (DNT), nicotinamide adenine dinucleotide (NADH), 3-(N-morpholino)propanesulfonic acid (MOPS) were purchased from Sigma-Aldrich. Others chemicals used in this work were of analytical grade or better and used as received without further purification.

2.2. Instrumentation

The X-ray diffraction patterns of powder samples (PXRD) were recorded using Philipps X-Pert Pro diffractometer with Cu K_α radiation source ($\lambda = 0.15405$ nm). Patterns were recorded over the 5–70° (2 θ) range in steps of 0.033° with a counting time of 200 s per step.

Infrared transmission spectra (FTIR) were recorded using the KBr pellet technique over a wavenumber region of 400–4000 cm⁻¹ with a Nicolet 5700 spectrometer from Thermo Scientific. The sample was mixed and homogenised with dry potassium bromide in a 1% of weight. Hydrodynamic diameter (d, nm) and zeta potential (ζ -potential, mV) were obtained for the pristine LDH samples and for the biohybrids by dynamic light scattering (DLS) and electrophoretic light scattering (ELS), respectively, using a Zetasizer Nano ZS instrument (Malvern Instruments) coupled to an automatic titration unit (MPT-2). The measurements were performed using buffered sample suspensions containing 0.05 M MOPS, pH 7.5.

Fluorescence spectra of the free and immobilized enzymes in aqueous solution (~ 0.1 mg / mL) were recorded at room temperature at $\lambda_{\text{exc}} = 280$ nm and $\lambda_{\text{em}} = 300$ -450 nm. A Varian Cary Eclipse fluorescence spectrophotometer was used, adopting a 5 nm bandpass on both excitation–emission. FESEM characteristics of the samples were imaged by a Zeiss supra 55 FEG-VP operating at 3 keV and 10 kV combined with an energy dispersive X-ray (EDX) analyzer. Transmission electron microscopy (TEM) images were recorded on a Hitachi 7650 microscope operated with an acceleration voltage of 80 kV. To perform the characterization, a drop of the suspension was deposited on a 400 mesh holey carbon-coated copper grid and dried at room temperature. AFM images were obtained on a Bruker Nanoscope IIIa atomic force microscope. Imaging was achieved using the repulsive mode in intermittent contact, commonly known as the “tapping” mode.

2.3. NfrA2/YncD expression and purification

The production and purification of the recombinant His-tagged NfrA2/YncD enzyme was obtained as previously described [26], with some modifications. Typically, *E. coli* BL21 (DE3) pLys cells carrying the recombinant plasmid were grown overnight at 30 °C in Luria-Bertani (LB) medium containing 100 µg/mL of ampicillin and 34 µg/mL of chloramphenicol, under agitation (140 rpm) on an orbital shaker. The expression of the enzyme was realized by induction at $OD_{600\text{ nm}} = 0.6$ with 1 mM of isopropyl β-D-1-thiogalactopyranoside (IPTG) and incubation of the culture at 30 °C overnight. Crude extracts were obtained by lysis of cells in a One Shot Cell Disrupter (Constants Systems), under 2.6 kbar pressure (3 cycles), in 50 mM sodium phosphate buffer solution (PBS), pH 8, containing 300 mM NaCl and 10 mM imidazole (7 mL/g of cells). Cell debris were eliminated by centrifugation (20000 g for 30 min at 4 °C) and the supernatant was loaded on a Ni²⁺-nitrilotriacetate agarose (Ni-NTA) chelating affinity column (Qiagen) previously conditioned with the same PBS. After washing the column with 50 mM PBS pH 8, containing 300 mM NaCl and 20 mM of imidazole at 4 °C, the His-tagged NfrA2/YncD was finally eluted with 50 mM PBS, pH 8, containing 300 mM NaCl and 250 mM imidazole. Fractions containing the enzyme were pooled and dialyzed overnight in 2 mM PBS pH 8. A second dialysis was carried out in deionized water for 5 h.

The size of the purified protein was monitored with SDS-PAGE molecular mass standards, between 10 and 250 kDa (BioRad). SDS-PAGE was performed in 12 % (w/v) polyacrylamide gel as described by Laemmli (1970) [33]. The SDS-PAGE showed a good expression of the protein with a major band in the purified extract corresponding to the monomer size of NfrA2/YncD as described by Carles et al. [26] (See supporting information Figure S2). The purified NR enzyme was lyophilized and the powder was stored at -18 °C until needed.

2.4. Enzyme activity assay

The protein content of free and immobilized enzyme samples was estimated by the Bradford assay [34], using a Coomassie blue-based protein dye reagent (BioRad) and BSA as the standard protein. Briefly, the Bradford reagent was added to a solution containing free (1-6 μg of protein) or immobilized NR (0.5-3 μg of protein), to a final volume of 20 % (w/w), and shook manually in a 96 - well microplate. In the case of the immobilized NR, the content of LDH was ≤ 2 % (w/v) in all the samples to ensure the complete dissolution of the material and release of the enzyme, maintaining the linearity of the microassay. After 10 min, the absorbance at 595 nm of the mixture was measured using a microplate reader (TECAN[®]) and compared to the BSA standard curve made in the same buffered conditions.

Enzyme activity of the NR for degrading 0.1 mM mesotrione was evaluated at 28 °C as previously described [26], in 50 mM MOPS, at optimum pH 6.5, in the presence of 0.7 mM NADH and 12.5 or 25 $\mu\text{g}/\text{mL}$ of free or immobilized enzyme, respectively. The reaction was stirred and stopped after 1 h by the addition of concentrated hydrochloric acid with final concentration of 7 % (v/v). The catalytic reaction was linear in the whole time interval. The disappearance of mesotrione was then monitored by HPLC as previously described [26]. One unit of nitroreductase activity (U) was defined as the amount of enzyme which transforms 1 μmol of mesotrione equivalent per minute under the above experimental conditions. Specific activity, expressed as units of enzyme per mg of protein (U/mg or $\mu\text{mol}/\text{min}\cdot\text{mg}$), was monitored during the different purification stages, until obtaining the lyophilized protein. The enzymatic activity was conserved during the whole process, with a purification index of 10.9 compared with the crude extract. Indeed, the specific activity of the crude extract was 2.4 mU/mg of protein and that of the purified NR was 25.4 ± 6.3 mU/mg protein.

When DNT was tested as a substrate, the enzymatic activity of free NR was determined *via* the consumption of NADH by spectrophotometry at 340 nm ($\epsilon_{340} = 6220 \text{ M}^{-1}\text{cm}^{-1}$) using a Cary 300

UV-Vis (Agilent). The reaction was carried out in 0.1 M PBS (pH = 6.5) containing 300 μM DNT, 350 μM NADH and 20 μg of NR. The specific activity was 2.99 U/mg protein (1 U = 1 μmol of NADH consumed/min).

2.5. Preparation of LDH samples

Two samples of nitrate-intercalated LDH compounds, namely MgAl-LDH and ZnAl-LDH, were prepared with 2:1 $\text{M}^{2+}/\text{M}^{3+}$ molar ratio by classical coprecipitation (see supporting information) [35]. MgAl-NO₃ nanoparticles (noted MgAl-LDH_{nano}) were prepared by flash coprecipitation, followed by a hydrothermal treatment as previously reported [36, 37]. A volume of 100 mL of metal nitrate solution (Mg/Al = 2, 0.4 M) was rapidly added to 300 mL of a 0.25 M NaOH solution under vigorous stirring. The dispersion was aged for 30 min at pH 10.0 in ice bath. The whole procedure was carried out under N₂ atmosphere. The dispersion obtained was hydrothermally treated at 150 °C and after 4 h, it was air-cooled. Then, the sample was centrifuged at 18500 g for 30 min, washed three times with deionized water and dispersed in 50 mL of deionised water. The resulting nanoparticles were re-dispersed in deionized water and stored as a colloidal dispersion (26 %, w/w) at 4 °C.

2.6. Immobilization of NR on LDH materials

In this study, two different immobilization strategies were investigated to prepare NR@LDH biohybrids, adsorption and direct coprecipitation, since it is well-known that immobilization step can strongly modify the enzyme activity [38]. NR was immobilized on MgAl-LDH, ZnAl-LDH and MgAl-LDH_{nano} materials by adsorption process, mixing enzyme and LDH suspensions. Suspensions of 2 mL of 50 mM MOPS pH 7.5, containing 2 mg of LDH and NR with initial concentrations (C_i) between 0.1 and 2 g/L were gently shaken at 30 rpm. After shaking overnight at 4 °C, the suspensions were centrifuged at 11000 g for 15 min, washed with deionized water several times and stored in 50 mM MOPS pH 7.5 at the same temperature. The NR adsorption

isotherm on MgAl-LDH_{nano} was performed and fitted to the linear form of Freundlich's equation, $C_s = K_f C_e^{N_f}$, and Langmuir-Freundlich's equation, $C_s = (C_m C_e^{m_f}) / (K_d + C_e^{m_f})$, as previously described [19].

Two biohybrids were prepared by the direct coprecipitation route following the method described above and performed in this case in presence of the enzyme NR in an adapted reduced scale material (see supporting information) [39]. In both cases, the amount of immobilized protein on the support (C_s) was quantified indirectly from the difference between the initial (C_i) and the equilibrium (C_e) solution concentrations of protein, respectively, through the following

$$\text{equation: } C_s = \frac{(C_i - C_e) \times V}{m} \quad (1)$$

where C_s (mg/g) is the amount of NR adsorbed, or adsorption capacity, at the equilibrium concentration C_e (mg/L); C_i (mg/L) is the initial protein concentration in solution; V is the solution volume (L) and m is the adsorbent mass (g). In addition, the amount of immobilized enzyme was also determined directly from the NR@LDH biohybrids using the Bradford assay as described above.

2.7. Storage stability and recyclability experiments

For storage stability, the biohybrids were stored at 4 °C in two forms: in solution (50 mM MOPS, pH 7.5) or as a lyophilized powder. The biocatalytic activity was compared with that of the free enzyme stored under the same conditions. The specific activity of the free or immobilized enzyme was checked during at least one month, using 0.1 mM mesotrione under the same assay conditions as those mentioned before. The pristine LDH was used as a negative control for catalytic activity toward mesotrione adsorption and degradation.

To study the effect of recovering and recycling the biocatalysts, a NR@LDH biohybrid sample was repeatedly exposed to mesotrione. The NR@LDH biohybrid (0.15 mg), with a protein loading of $C_s = 0.6$ mg/mg MgAl-LDH_{nano}, was added to the reaction medium (1 mL) containing

100 μM mesotrione and 700 μM NADH in 50 mM MOPS pH 6.5 at room temperature. The NR@LDH biohybrid was recovered by centrifugation in the same reaction vials (1.5 mL eppendorf tubes) and used immediately in a new reaction cycle. Then, a volume of 0.1 mL of concentrated hydrochloric acid was added to 0.5 mL of supernatant and the NR activity was determined as described in the previous section. The reaction was then repeated 3 additional times resulting in 4 sequential cycles of the same NR@LDH sample.

2.8. Electrochemical experiments

Cyclic voltammetry (CV) was recorded out with a three-electrode system using a PGSTAT 204 controlled by the NOVA software (Metrohm). A saturated calomel electrode (SCE) was used as the reference electrode and a Pt wire as the counter electrode. The working electrode was a modified glassy carbon electrode (GCE, $A = 0.196 \text{ cm}^2$). Before the deposition of the NR@MgAl-LDH_{nano} biohybrid, the GCE was polished with a diamond paste (1 μm), washed with acetone, then polished with alumina slurry (0.04 μm), and finally rinsed with ethanol and water. A drop (50 μL) of NR@MgAl-LDH_{nano} mixture, corresponding to 100 μg of biohybrid material (Enzyme/LDH 1:1) was deposited on the surface of GCE and the bioactive layer was allowed to dry under vacuum for 1 h. Before use, the NR@MgAl-LDH_{nano}/GCE modified electrodes were rehydrated in 0.1 M PBS (pH = 6.5) for 15 min and then transferred into the electrochemical cell containing 0.2 mM mesotrione or DNT and 0.4 mM NADH in 0.1 M PBS to carry out CV experiments at a scan rate of 10 mV/s under argon atmosphere.

3. RESULTS AND DISCUSSION

3.1. Synthesis and biological activity of NR@LDH biohybrids

In this study, purified NfrA2/YncD from *Bacillus megaterium* Mes11, noted NR, was immobilized on nitrate-intercalated MgAl-LDH and ZnAl-LDH biocompatible matrices by two different approaches: adsorption and coprecipitation leading to biohybrids named NR@LDH-ads

and NR@LDH-cop, respectively. According to the literature and our previous studies concerning enzyme immobilization on LDH-type materials [17, 20], the initial M^{2+}/M^{3+} ratio in the LDH layer was fixed at 2 in order to maximize the charge density of the layers of these materials. Nevertheless, other key parameters were optimized: a) the type of the immobilization procedure, b) the chemical composition of the LDH and c) the enzyme/LDH mass ratio ranging from 0.1 to 2.

For the adsorption, three different LDH samples were prepared either by the classical method of coprecipitation [35], ZnAl-LDH and MgAl-LDH, or flash coprecipitation MgAl-LDH_{nano} [36, 37] to tune the particle size and aggregation state. All the samples prepared exhibited the typical XRD patterns of hydrotalcite-like materials (Figure 1) with a basal spacing d of 0.86 nm in agreement with the intercalation of nitrate anions between the LDH layers (See supporting information Table S2). The chemical analyses confirmed the LDH coprecipitated with a M^{2+}/M^{3+} ratio near the expected one, with values of 2.2, 2.0 and 1.9 for ZnAl-LDH, MgAl-LDH and MgAl-LDH_{nano}, respectively.

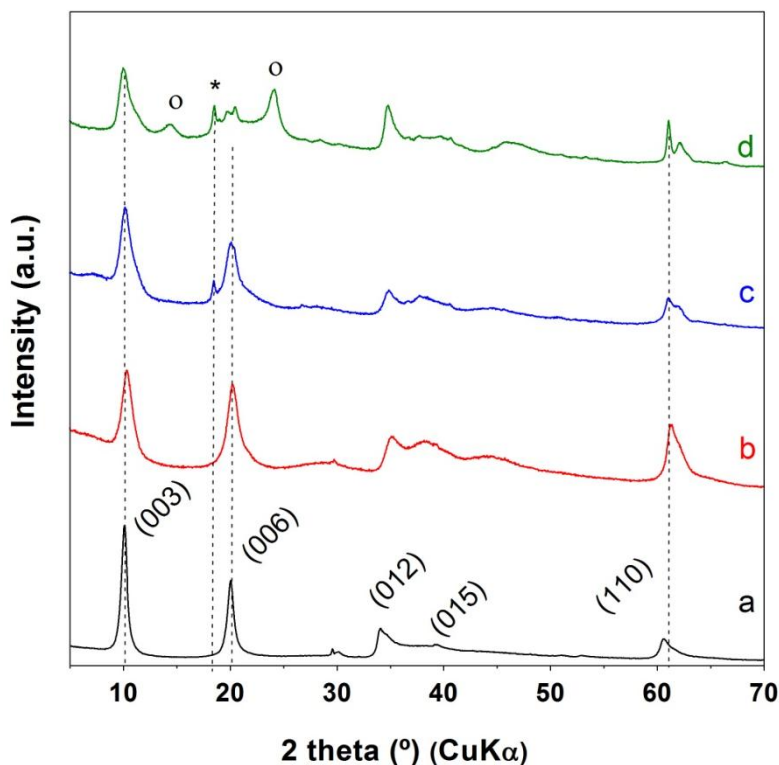


Figure 1. XRD patterns of a) ZnAl-LDH b), MgAl-LDH c) MgAl-LDH_{nano} and d) NR@MgAl-LDH_{nano} at Cs = 0.6 mg/mg (* Mg(OH)₂).

The TEM images (Figure 2) of the precursors further reveal the differences between the two synthetic routes used, in relation to their morphology and particle size. The samples prepared by the classical method of coprecipitation, MgAl-LDH and ZnAl-LDH, present the usual densely packed particles, configured as aggregates (Figures 2A-2B). In contrast, small polydisperse particles with an almost spherical shape are observed for the MgAl-LDH_{nano} sample (Figure 2C). The particle sizes deduced from the TEM images range from 70 to 130 nm, with an average around 90 nm. This value is close to the hydrodynamic diameter of 130 ± 54 nm (polydispersity index: 0.17) obtained by DLS. In the case of samples prepared by classical coprecipitation, greater particle size about 600-700 nm was inferred.

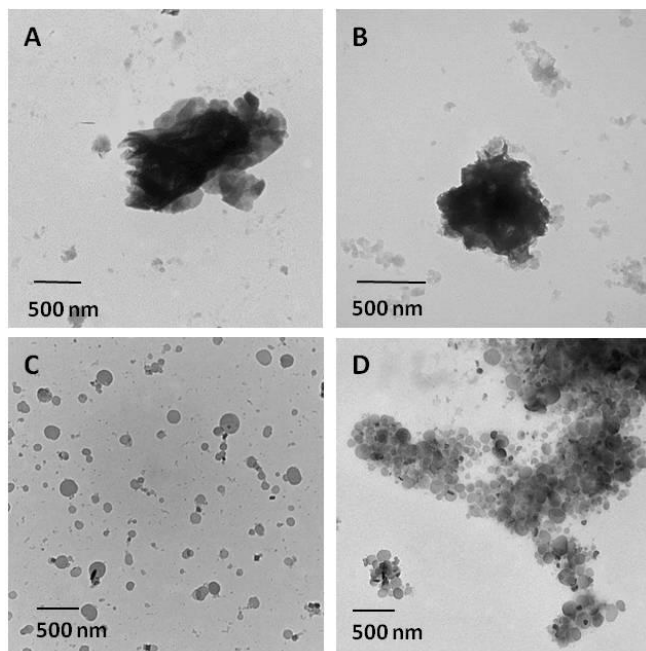


Figure 2. TEM images of A) ZnAl-LDH B), MgAl-LDH C) MgAl-LDH_{nano} and D) NR@MgAl-LDH_{nano} at $C_s = 0.6$ mg/g.

A key factor leading to the immobilization of proteins on LDH and other inorganic materials is the electric charge parameters [40]. As expected, the zeta potential values for all the LDH matrices are positive ranging from 21 mV to 37 mV at a pH of 7.5 (see supporting information Table S.2). For NR, the isoelectric point (IEP) was determined at pH 5.7 (See supporting information Figure S3) close to the theoretical IEP = 6.1 calculated on the basis of the amino acid sequence of NfrA2/YncD from *B. megaterium* [41, 42]. Considering this IEP, the protein will be negatively charged at basic pH (50 mM MOPS, pH 7.5) used in the immobilization process. A priori, these opposite values should favour electrostatic interactions between both components and promote the biohybrid formation [12, 19, 20].

Figure 3A shows the influence of the chemical composition of the LDH (MgAl vs ZnAl), prepared by classical or flash coprecipitation, on the immobilization yields and the enzyme activity of the NR immobilized by adsorption or coprecipitation at different NR loadings.

Concerning the immobilization yield, the enzyme was completely immobilized for the lower enzyme amount (Enzyme/LDH initial mass ratio: $Q = 0.5$), proving an excellent immobilization efficiency in all the cases. At $Q \geq 1$, modulations were observed according to the matrices and conditions used. The amount of immobilized enzyme in the NR@ZnAl-LDH-ads biohybrid was close to 100 % for the whole Q range studied, while in the NR@MgAl-LDH-ads it significantly decreased with the increase of the Q ratio, evidencing the material saturation. Such influence of the LDH chemical composition on the enzyme immobilization rate was previously observed for transketolase and alkaline phosphatase using MgAl-LDH and ZnAl-LDH as supports [17, 38]. However, the immobilization capacity of the inorganic materials was not only influenced by its chemical composition but also by the immobilization method: for instance, the amount of immobilized enzyme on the MgAl-LDH matrix was significantly higher when the coprecipitation route was used as an alternative immobilization strategy (NR@MgAl-LDH-cop biohybrid). Obviously, the coprecipitation process overcomes the limitation of the adsorption surface area, promoting a high immobilization yield and favouring the dispersion of the biomolecule within the solid phase [43, 44]. Charradi et al. [45] also observed the increase effect of the immobilization yield of the heme protein hemoglobin on Mg₂Al-LDH compounds prepared by coprecipitation. However, a different result was observed after the immobilization of transketolase on Mg₂Al and Zn₂Al-LDH inorganic supports, where the adsorption process yielded to a high enzyme immobilization compared with the *in situ*-coprecipitation [38]. As mentioned above, electrostatic or coulombic interactions due the opposite surface charge values promoted the stable assembly of LDH enzymes and a high performance of NR immobilization. The higher NR immobilization by adsorption displayed by the ZnAl-LDH sample may be related to the different specific buffering properties due to a lower surface basicity of the sample ZnAl-LDH compared with the MgAl-LDH matrix [17, 38, 46].

In parallel, the biohybrid performance toward mesotrione biodegradation as a function of Q was also investigated (Figure 3B). The free enzyme exhibited a specific activity for mesotrione biotransformation of ≈ 25 mU/mg protein. Systematically, the enzyme immobilization induced a decrease of the enzymatic activity. An activity loss compared with the free enzyme has been commonly observed in non-specific adsorption processes of enzymes randomly bound to solid surfaces, especially in the so-called “soft” proteins [17, 19, 45, 47-49]. However, a better catalytic performance for the samples based on NR immobilized on MgAl-LDH matrices by adsorption was systematically observed, showing an increase of the specific NR activity higher than 4-fold compared with NR immobilized on the ZnAl-LDH phase at an enzyme/LDH initial mass ratio $Q = 1$. As mentioned above, this trend could be due to the difference of surface properties for these two LDH chemical compositions as already observed in the literature [17]. It is noteworthy that the strategy for the NR immobilization had a greater influence in the final performance of the biohybrids. The NR immobilized by coprecipitation, NR@MgAl-LDH-cop, significantly decreased its activity performance compared with the NR@MgAl-LDH-ads, probably due to the pH instability of this enzyme at $\text{pH} = 9$ used for the biohybrid synthesis. Indeed, at this basic pH, the free enzyme activity dropped by 90 % after 3 h, meanwhile the free enzyme fully retained its activity at $\text{pH} 7.5$ in 50 mM MOPS for several days. Conversely, the LDH particle size had not a noticeable influence in the final performance of the biohybrids. However, the data obtained using the MgAl-LDH sample, prepared by classical coprecipitation, were poorly reproducible and rather heterogeneous, probably due to the greater particle size distribution of this sample.

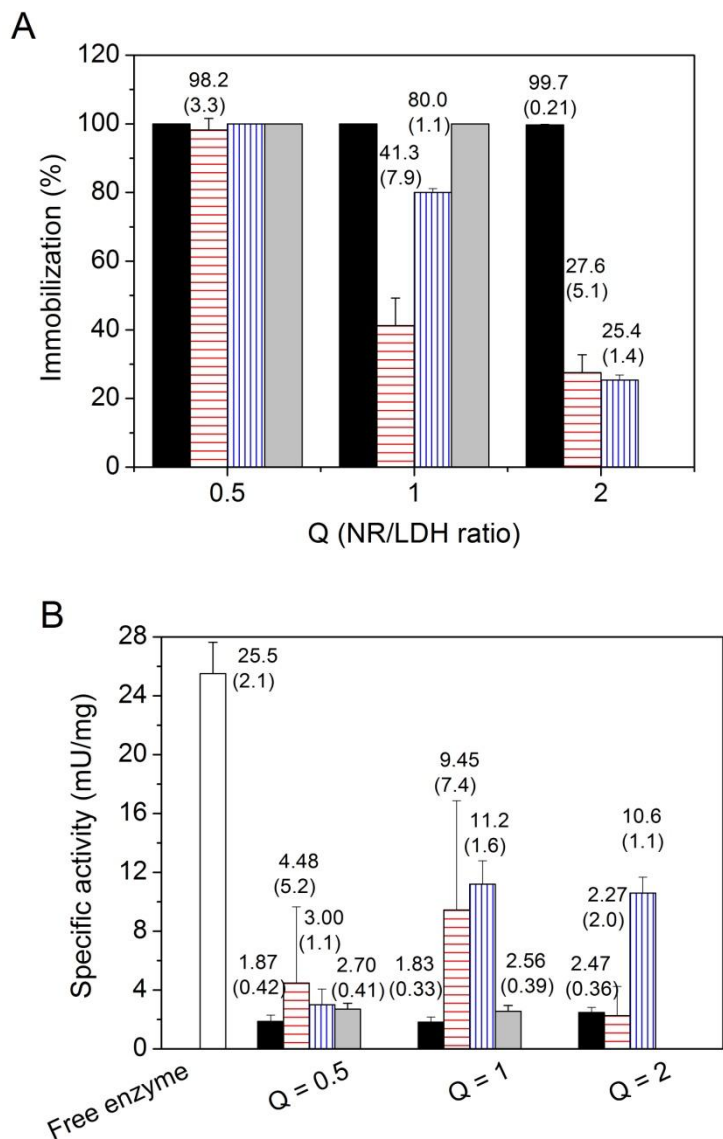


Figure 3. Immobilization yield (A) and activity performance (B) of the NR@LDH biohybrids: NR@ZnAl-LDH-ads (black), NR@MgAl-LDH-ads (red horizontal lines), NR@MgAl-LDH_{nano} (blue vertical lines) and NR@MgAl-LDH-cop (grey) at different Q values (experiments run in triplicate).

In summary, the results highlight the complexity of the immobilization process of enzymes on LDH inorganic materials which strongly depends on the inherent properties of the enzyme-LDH biosystem selected and the immobilization strategy which determine the interactions between the

two components. The NR immobilization on the MgAl-LDH_{nano} matrix by adsorption at NR/LDH initial mass ratio $Q = 1$ exhibited a good immobilization yield (80 %) and the best catalytic activity (44 %) compared to free enzyme with a good reproducibility of the immobilization process (RSD < 1.5 %). Consequently, the NR@MgAl-LDH_{nano} system was further investigated for a better understanding of the immobilization process and biohybrid performance.

3.2. Physico-chemical and structural characterization of NR@MgAl-LDH_{nano}

Figure 4A displays the adsorption isotherm of the NR on the MgAl-LDH_{nano} which corresponds to an H-type shape, according to the classification reported by Giles et al. [50]. Similarly, the enzymatic activity increased with the amount of immobilized NR, following a similar pattern. As proposed in a previous study [19], an adequate description of the protein adsorption process on LDH compounds can be obtained by the non-linear fitting of the adsorption isotherm to the Freundlich model and the composite Langmuir-Freundlich model. Both models offered a good fit to the adsorption isotherm data (Table 1). However, the Langmuir-Freundlich equation was somewhat more adequate to describe the general process of NR adsorption, showing C_m values close to those obtained experimentally. The K_f and K_d parameters are characteristic of systems with strong interactions between both components involved in the adsorption process, i.e. the enzyme and the support. The n_n values higher than 1 and the N_f values close to 0, clearly suggested a positive cooperativity in binding and a heterogeneous nature of the enzyme adsorption [51]. This may indicate that the increase of NR adsorbed on the LDH is favoured by attractive forces due to lateral enzyme-enzyme interactions, as observed for another enzyme/LDH system [19].

The “high affinity” isotherm could be attributed to the existence of electrostatic interactions, considering the opposite charge values of both components at slightly basic experimental pH 7.5. Indeed at this pH, the amount of NR adsorbed led to a marked negative progression on the

surface charge of the nanomaterial, from a positive zeta potential (ζ) value of the pristine LDH (+35 mV) to ζ values close to that of the free enzyme (Figure 4B). Additionally, this charge inversion, together with the increase of the biocatalytic activity with the enzyme loading, demonstrated the successful immobilization of the NR on the MgAl-LDH_{nano} sample.

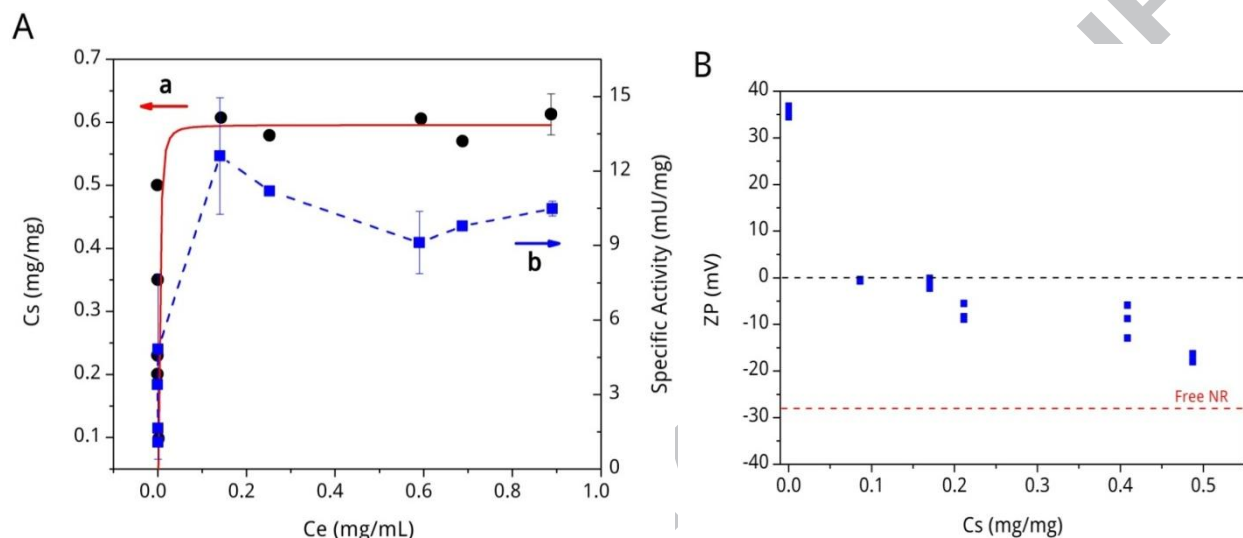


Figure 4. A) Non-linear fit of the adsorption isotherm of NR on MgAl-LDH_{nano} using the Langmuir-Freundlich model (red curve; a), and NR specific activity (blue curve; b) and B) evolution of the ζ with the enzyme loading (experiments run in triplicate). Red dot line: ζ value of the free enzyme (50 mM MOPS, pH 7.5 and 25 °C).

Table 1. Freundlich and Langmuir-Freundlich parameters for NR adsorption on MgAl-LDH_{nano}

Freundlich model			Langmuir-Freundlich model			
K_f	N_f	R^2	C_m	K_d	n_{lf}	R^2
0.69 ± 0.08	0.20 ± 0.08	0.92	0.59 ± 0.15	5316 ± 540	1.74 ± 0.55	0.99

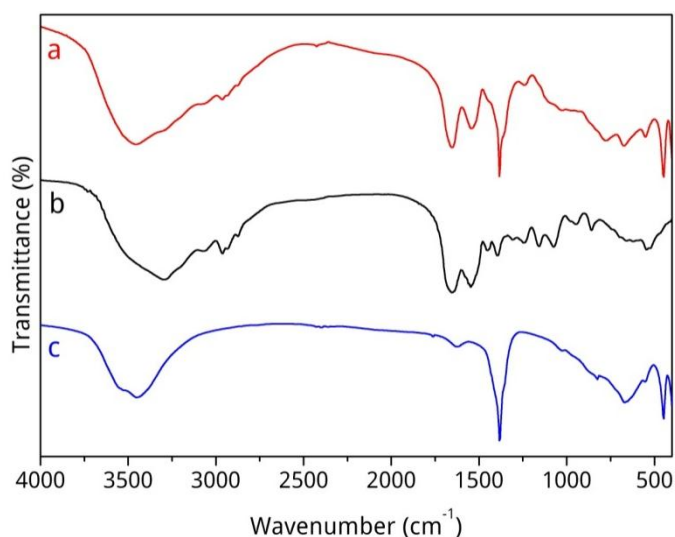
The XRD pattern of the NR@MgAl-LDH_{nano} biohybrid (Figure 1) confirms the preservation of the well-crystallized LDH structure after the enzyme adsorption. The d spacing remains the same

compared to the pristine MgAl-LDH_{nano} material, suggesting that nitrate is the main interlayer anion and no intercalation of the NR occurred. Nevertheless, after the adsorption, the reflections of the side Mg(OH)₂ phase already observed in the precursor MgAl-LDH_{nano} are still present conjointly with two additional reflections at 14.4° and 24.0° which could correspond to the partial intercalation of an anionic species from the buffer adsorption medium. Vibration bands typical of both LDH-type and the enzyme structure are systematically observed by FTIR spectroscopy in the NR@MgAlLDH_{nano} biohybrid sample (Figure 5A), confirming the presence of adsorbed enzyme on the LDH material. The characteristic broad stretching vibration band at ca. 3500 cm⁻¹ ($\nu_{\text{O-H}}$) is attributed to OH groups of interlayer water molecules and the hydroxylated brucite-layers. The vibration bands ranging between 400 and 800 cm⁻¹ were assigned to the $\nu_{\text{M-O}}$ and $\bar{\delta}_{\text{O-M-O}}$ lattice vibrations. Additional bands characteristic of the $\nu_{\text{C-H}}$ and amide vibration bands of the enzyme are present at 2750 cm⁻¹ and 800-1700 cm⁻¹. Noticeably, the intensity of the band attributed to $\nu(\text{NO}_3)$ at 1387 cm⁻¹ in the biohybrid and LDH material slightly decreased but was still present indicating that nitrate-intercalated LDH remains as the main LDH phase after the immobilization of the enzyme which adsorbed at the particle surface rather than by intercalation in the interlayer space. This result is in agreement with those observed previously for enzyme adsorption using LDH matrices [20, 52].

We further investigated aqueous suspension of NR@MgAl-LDH_{nano} biohybrids by fluorescence spectroscopy and compared the spectra with that of the native enzyme in order to obtain information about the immobilization effect on the structural compactness and unfolded state of NR (Figure 5B). In fact, fluorescence characteristics of the aromatic amino acid residues of enzymes, such as tryptophan (Trp) or tyrosine (Tyr), are valuable parameters to evaluate conformational changes upon enzyme immobilization [53, 54]. When excited at $\lambda_{\text{exc}} = 280$ nm, free NR displayed a maximum fluorescence emission at 339 nm, close to the maximum emission

produced by the amino acid residue Trp (350 nm). Once immobilized, the NR fluorescence spectra changed with the enzyme loading into the NR@MgAl-LDH_{nano} biohybrids. At low enzyme loading values, the fluorescence yield decreased and a new peak at red wavelength values was clearly observed. These results suggest a change in the local environment polarity of the fluorophore residues of the immobilized enzyme which became more accessible to the solvent molecules compared to the native NR, as a consequence of the compactness relaxation of the enzyme structure. Similar results have been reported in the literature for the immobilization of amylase for instance using LDH as support [15, 19, 55]. However at higher saturation loading ($C_s = 0.62$ mg/mg), the emission spectrum was similar to that of the free enzyme, highlighting that in the NR case, this effect was reduced at saturated enzyme loading values.

A



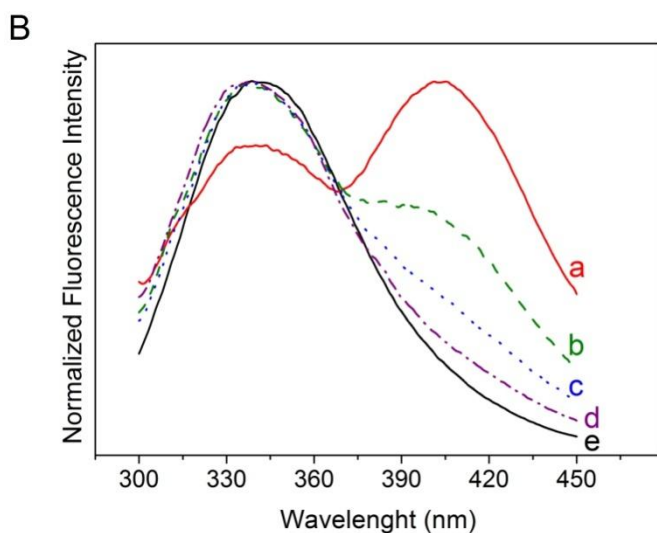


Figure 5. A) FT-IR spectra of the NR@MgAl-LDH_{nano} biohybrid ($C_s = 0.6$ mg/mg) (a), free NR (b), and pristine LDH (c). B) Fluorescence emission spectra of the colloidal suspension of NR@MgAl-LDH_{nano} biohybrids with different enzyme loading: $C_s = 0.2$ mg/mg (a), $C_s = 0.4$ mg/mg (b), $C_s = 0.57$ mg/mg (c), $C_s = 0.62$ mg/mg (d), and the free enzyme (e). Excitation at $\lambda_{exc} = 280$ nm.

This likely modification in enzyme configuration due to its immobilization can have a consequence on its catalytic activity. Therefore, we analysed the evolution of the enzymatic activity of the biohybrids as a function of the enzyme loading (C_s) (Figure 6). As mentioned above, the activity of the biohybrids increased with the increase of immobilized enzyme. This increase reaches a maximum value of ca. 5 mU/mg biohybrid. As shown in the Figure 6 (blue curve b), higher activity performance of the NR@MgAl-LDH_{nano} biohybrids, defined as NR specific activity (mU/mg NR) per mg of enzyme loaded on the support (C_s), was observed when the saturation in terms of enzyme adsorption was achieved ($C_s = 0.55 - 0.6$ mg/mg). These values correspond to initial concentrations of NR in solution higher than $C_i > 0.8$ mg/mL of NR.

It is well-known that the coverage of proteins non-specifically adsorbed on solid surfaces frequently results in conformational and/or orientational changes within the adsorbed surfaces affecting its bio-activity [51, 56]. After the attachment step, the biomolecule tends to optimize its interactions with the surface of the LDH which usually leads to some degree of spreading specially for the so-called “soft” proteins, inducing the conformational modification previously observed by fluorescence spectroscopy on the NR@MgAl-LDH_{nano} biohybrids (Figure 5B). This energy minimization due to the enzyme spread across the surface may negatively affect the biocatalytic performance, explaining the decrease of its efficiency at low load values. On the other hand, the structure relaxation of the biomolecule strongly depends on the available adsorption sites [57]. The number of adsorption sites is reduced with the incorporation of more biomolecules to the surface and new enzyme-enzyme interactions arise in the system. Therefore, the configuration set at high load values better preserved the native NR conformation and then enhanced the performance of the biocatalyst [58].

For the α -amylase/LDH system [19] an optimal configuration was observed at average load values but an enzyme aggregation occurred at high load values, decreasing the specific activity of the biocatalyst. However, this multilayer adsorption effect is unlikely to occur with the NR@MgAl-LDH_{nano} system since a single plateau was observed on the adsorption isotherm (Figure 4A).

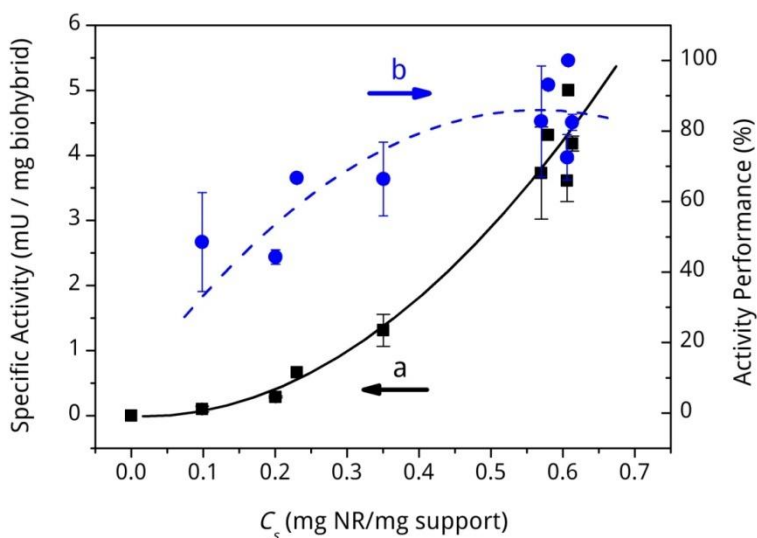


Figure 6. Effect of NR loading on the specific enzyme activity (a) and performance (b) of the NR@MgAl-LDH_{nano} biohybrids (experiments run in triplicate).

3.3 Recyclability and storage stability of the NR@MgAl-LDH_{nano} biohybrid

Usually in biohybrid materials, the immobilization of enzymes may allow their reuse and may increase their catalytic productivity reducing the overall cost associated with the enzyme production in industrial bioprocesses or biotechnology development. Thus, we explored here the recovering and recycling effect on the catalytic performance of NR@MgAl-LDH_{nano} biohybrid ($C_s = 0.6$ mg/mg) toward the biodegradation of mesotrione. Figure 7A shows the evolution of the relative activity of the NR@MgAl-LDH_{nano} biohybrid during 4 cycles of reuse. Although a partial loss of biocatalytic activity was observed at each step, from 80 % to 60 % of the catalytic activity was retained with respect to the immediately previous cycle, achieving ca. 30 % of activity retained after 4 cycles of reuse. Since no appreciable release of enzyme was detected in the supernatant between each cycle, such a loss of enzymatic activity could be related to a NR denaturation during the recycling process.

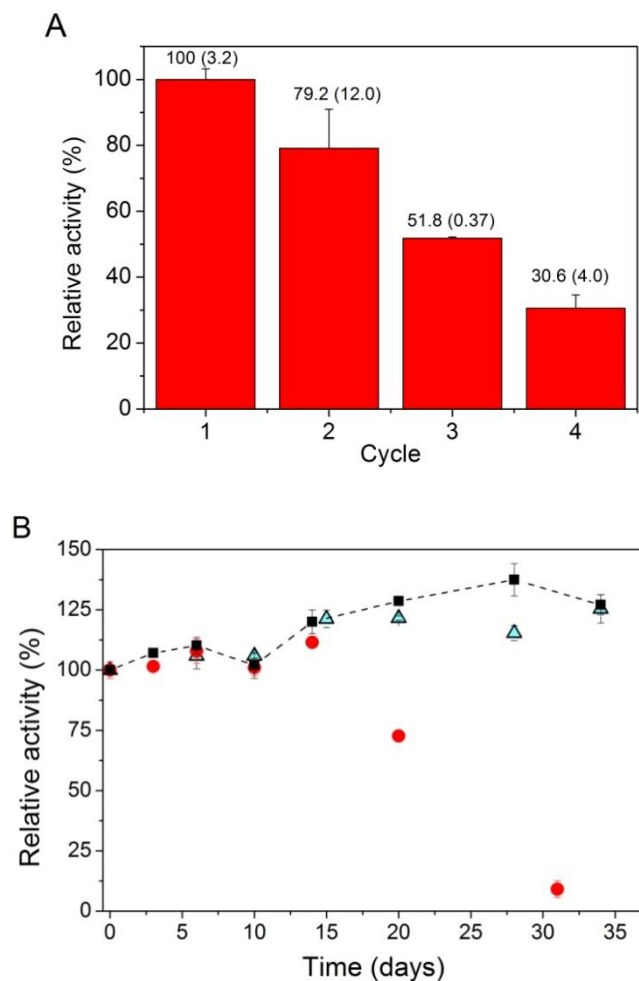


Figure 7. A) Recyclability of the NR@MgAl-LDH_{nano} biohybrid ($C_s = 0.6$ mg/mg) using $100 \mu\text{M}$ of mesotrione in 50 mM MOPS pH $6.5 + 0.7$ mM NADH, and 40 min of reaction time by cycle (experiments run in triplicate). B) Relative NR activity with time of the lyophilized extract of the free native NR (black squares), a suspension of NR@MgAl-LDH_{nano} biohybrid in 50 mM MOPS (red circles) and the lyophilized NR@MgAl-LDH_{nano} biohybrid (blue triangles). Samples were stored at 4°C .

Another important point concerns the storage of biohybrid materials in the dry state. It provides several advantages for enzyme-based materials such as preventing enzyme leakage in long-term storage, avoiding the degradation of the enzyme by microbiological activity or

undesirable side-reactions, and improving the handling and transportation. For that, we evaluated the activity of NR@MgAl-LDH_{nano} biohybrid after lyophilisation (Figure 7B). The lyophilized form of this biohybrid retained full activity after its rehydration in comparison with its un-dried form. This result suggests that the different steps involved in the lyophilization treatment did not affect significantly the performance of the biohybrid material. Furthermore, the storage stability of the immobilized enzyme with time was investigated in comparison with that of the lyophilized free native enzyme. NR@MgAl-LDH_{nano} biohybrids were studied in both stored forms at 4 °C, that is, as a suspension in MOPS (pH 6.5) and as a lyophilized powder. According to the results, the biohybrid in suspension retained its activity during 15 days, but a gradual activity loss was detected after. Nevertheless, the activity was fully maintained with the lyophilized biohybrid, at least for more than one month of storage. Surprisingly, an increase in the enzymatic activity was systematically observed after 10 days of storage for both lyophilized NR and lyophilized NR@MgAl-LDH_{nano} biohybrid and even for the biohybrid maintained in suspension. Such behaviour could be link to a slight structural change of the NR in solution with time, further experiments will be necessary to confirm it.

3.4. Electrochemical response of NR@MgAl-LDH_{nano} modified electrode

In order to test the suitability of NR-based biohybrids for biotechnology applications, such as biosensors, thin films were prepared using the NR@MgAl-LDH_{nano} biohybrid through a one-step deposition on a polished glassy carbon electrode. The surface morphology of the biohybrid film was explored by SEM and AFM measurements (Figure 8). Clearly, the surface of the film is homogeneous and continuous. The SEM high magnification image and AFM top view image allow us to distinguish the individual LDH nanoparticles involved into the dense biohybrid film with particle size in good agreement with the results obtained by DLS.

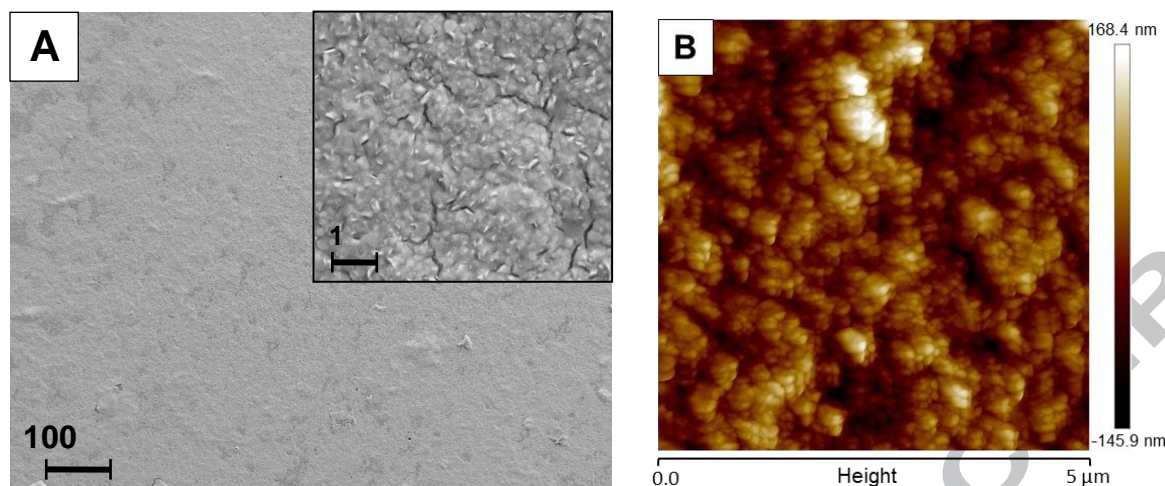


Figure 8. A) FE-SEM and B) AFM images of the NR@MgAl-LDH_{nano} film.

Enzymatic activity of the NR@MgAl-LDH_{nano} films was analysed by cyclic voltammetry (CV). In fact, the first step of the enzymatic mesotrione transformation by NR, in the presence of its cofactor NADH, leads to the formation of a hydroxylamino intermediate [26], which can be detected in electrochemistry at a potential of 0.3 V/SCE [59]. AMBA, the final metabolite of the enzymatic mesotrione degradation [26] can also be oxidized at a GCE (See supporting information Figure S4). Unfortunately, its oxidation potential (1.1 V/SCE) is more anodic than the oxidation potential of the NADH cofactor (0.7 V/SCE) [60]. Therefore, the electrochemical detection of AMBA cannot be taken under consideration in NR-based amperometric biosensors. The potential window for CV was therefore fixed between -0.3 and +0.5 V/SCE to prevent, with the lower potential limit, the direct electrochemical reduction of mesotrione and, with the higher limit, the electrochemical oxidation of NADH. Figure 9 shows the evolution of the CV curves when 0.4 mM NADH was added in a 0.2 mM mesotrione solution. The appearance of a small oxidation peak at +0.30 V/SCE, corresponding to the formation of hydroxylamino intermediate, confirms that the enzymatic reaction takes place at the modified electrode surface. However, the peak intensity was very low ($0.89 \mu\text{A cm}^{-2}$) for a 0.2 mM mesotrione concentration, evidencing a NR@MgAl-LDH_{nano} modified electrode not very sensitive to detect mesotrione, mainly due to the

low specific activity of the enzyme for this substrate (25 mU/mg and $K_M = 68 \mu\text{M}$) [26]. In the literature, it was reported that nitroreductases are effectively reducing various nitro-compounds [61]. For instance, we found that NR has a specific activity of 2.99 U/mg and a K_M value of 21 μM for dinitrotoluene (DNT). Therefore, DNT was a better substrate to test the electrochemical activity of the NR@MgAl-LDH_{nano} modified electrode. Figure 7B clearly shows a catalytic oxidation peak of 11 $\mu\text{A cm}^{-2}$ at +0.15 V/SCE when 0.2 mM DNT was reduced using this electrode in the presence of NADH. Similarly, Caygill et al. [62], described that the presence of nitroreductase NfsA from *E.coli* into the electrolyte improves the electrochemical detection of TNT and DNT at a screen-printed electrode, due to an increase of current magnitude of the oxidation peak of hydroxylamine.

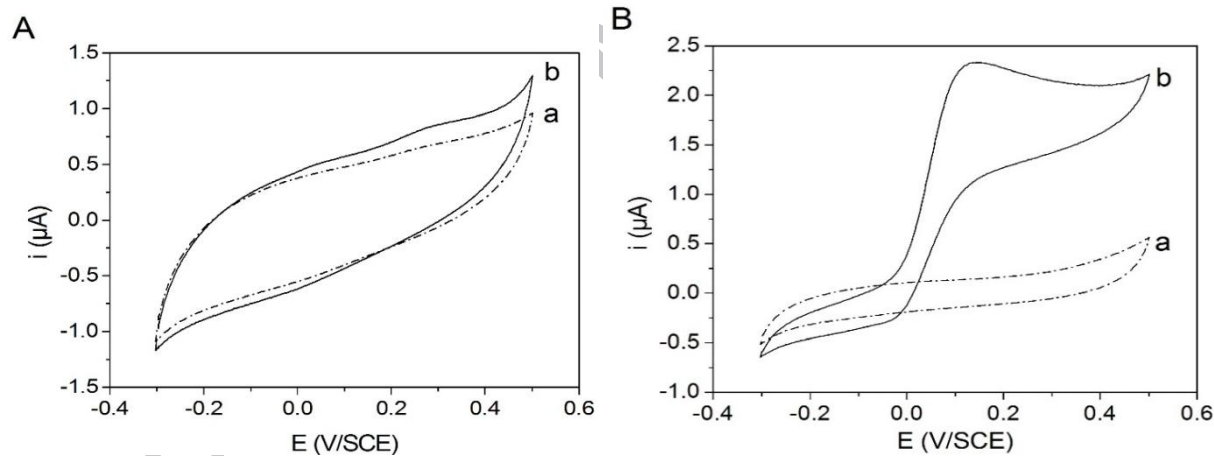


Figure 9. Cyclic voltammograms of (A) 0.2 mM mesotrione and (B) 0.2 mM DNT at NR@MgAl-LDH_{nano}/GCE without (a) and in presence of 0.4 mM NADH (b) (0.1 M PBS pH 6.5, $v = 10 \text{ mV/s}$).

4. CONCLUSIONS

Biohybrids containing nitroreductase (NR) and layered double hydroxide (LDH) particles were obtained by adsorption process and direct coprecipitation. Two distinct LDH chemical compositions were tested by modifying the nature of the divalent metal (Mg^{2+} or Zn^{2+}) involved within the layer while the LDH particle size and aggregation were varied according to the LDH synthesis process used. Analysis of the NR immobilization percentage and the retained activity revealed that the NR adsorbed on LDH nanoparticles (noted NR@MgAl-LDH_{nano}) in a ratio NR/LDH of $Q = 1$ gave the best results with 80 % of immobilized NR and 44 % of retained activity in comparison with the free native enzyme. The adsorption isotherm evidenced a strong affinity between the enzyme and the LDH nanoparticles further supported by the TEM images and zeta potential evolution. Remarkably, the highest activity performance of NR@MgAl-LDH_{nano} biohybrids was observed at the saturation *plateau* corresponding to $C_s \sim 0.6$ mg/mg, due to a better conservation of the native conformation of the immobilized enzyme. After 4 cycles of reuse, the NR@MgAl-LDH_{nano} biohybrid still retained 30 % of its initial biological activity, meanwhile the biological activity was fully maintained using the lyophilized biohybrid, at least after one month of storage. This work represents the first example of using LDH to immobilize NR leading to smart functional biohybrid with promising applications in diverse fields.[63]

Our preliminary results using CV evidenced that the enzymatic reaction takes place at an electrode surface modified by NR@MgAl-LDH_{nano}. While NR@MgAl-LDH_{nano} modified electrode was efficient to detect DNT, it appears not very sensitive for mesotrione due to the low specific activity of NR for this substrate. Further studies are currently under investigation to find another transduction strategy to develop a biosensor for mesotrione, based on NR@MgAl-LDH_{nano} more sensitive than sensors using clay based materials.[59] Since NR@MgAl-LDH_{nano} modified electrode is efficient to detect DNT, it should also be of great interest for detection of

other contaminants of emerging concern containing nitroaromatic moiety such as the antibiotics metronidazole and nitrofurazone which are both substrates of NR.[26]

5. ASSOCIATED CONTENT

Supporting Information

LDH synthetic conditions, SDSPAGE of the different recombinant *E. coli* BL21(DE3) pLys extracts, zeta potential curve of the His-tagged NfrA2/YncD as a function of the pH, cyclic voltammograms of AMBA at bare GCE and the unit cell parameters and zeta potential values at pH 7.5 of the LDH samples.

6. AUTHOR INFORMATION

Corresponding Author

*E-mail: vanessa.prevot@uca.fr

Author Contributions

The manuscript was written through contributions of all authors. All authors have given approval to the final version of the manuscript.

Notes

The authors declare no competing financial interest.

7. ACKNOWLEDGMENTS

The authors acknowledge Slim Hdiouech for his contribution in the electrochemical measurements. Authors acknowledge the Regional Auvergne Council, CNRS, the French

Ministry for Higher Education and Research and the European Regional Development Fund for financial support. We would also like to express our gratitude to the Clermont Environmental Research Federation, UBP/CNRS FR 3467/INRA.

8. REFERENCES

- [1] C. Spahn, S.D. Minter, *Enzyme Immobilization in Biotechnology, Recent Patents on Engineering*, 2 (2008) 195-200.
- [2] U. Guzik, K. Hupert-Kocurek, D. Wojcieszńska, Immobilization as a Strategy for Improving Enzyme Properties-Application to Oxidoreductases, *Molecules*, 19 (2014) 8995.
- [3] R. Singh, M. Kumar, A. Mittal, P.K. Mehta, Microbial enzymes: industrial progress in 21st century, *3 Biotech*, 6 (2016) 174.
- [4] S.A. Ansari, Q. Husain, Potential applications of enzymes immobilized on/in nano materials: A review, *Biotechnology Advances*, 30 (2012) 512-523.
- [5] C.-K. Lee, A.-N. Au-Duong, *Enzyme Immobilization on Nanoparticles: Recent Applications., Emerging Areas in Bioengineering*, Wiley-VCH Verlag GmbH & Co. KGaA, Weinheim, Germany, 2018, pp. 67-80.
- [6] R.A. Sheldon, *Enzyme Immobilization: The Quest for Optimum Performance, Advanced Synthesis & Catalysis*, 349 (2007) 1289-1307.
- [7] P. Zucca, E. Sanjust, *Inorganic Materials as Supports for Covalent Enzyme Immobilization: Methods and Mechanisms, Molecules*, 19 (2014) 14139.
- [8] P. Zucca, R. Fernandez-Lafuente, E. Sanjust, Agarose and Its Derivatives as Supports for Enzyme Immobilization, *Molecules*, 21 (2016) 1577.
- [9] J. Xu, J. Sun, Y. Wang, J. Sheng, F. Wang, M. Sun, Application of Iron Magnetic Nanoparticles in Protein Immobilization, *Molecules*, 19 (2014) 11465.
- [10] V.E. Bosio, G.A. Islan, Y.N. Martínez, N. Durán, G.R. Castro, Nanodevices for the immobilization of therapeutic enzymes, *Critical Reviews in Biotechnology*, 36 (2016) 447-464.
- [11] S. Datta, L.R. Christena, Y.R.S. Rajaram, Enzyme immobilization: an overview on techniques and support materials, *3 Biotech*, 3 (2013) 1-9.
- [12] C. Forano, S. Vial, C. Mousty, Nanohybrid enzymes - layered double hydroxides: potential applications, *Current Nanoscience*, 2 (2006) 283-294.
- [13] S. Vial, C. Forano, D. Shan, C. Mousty, H. Barhoumi, C. Martelet, N. Jaffrezic, Nanohybrid-layered double hydroxides/urease materials: Synthesis and application to urea biosensors, *Mater. Sci. Eng., C*, 26 (2006) 387-393.
- [14] M. Halma, A. Khenifi, M. Sancelme, P. Besse-Hoggan, P.-O. Bussière, V. Prévot, C. Mousty, Thin bacteria/Layered Double Hydroxide films using a layer-by-layer approach, *J. Colloid Interface Sci.*, 474 (2016) 151-158.
- [15] Z. An, S. Lu, J. He, Y. Wang, Colloidal Assembly of Proteins with Delaminated Lamellas of Layered Metal Hydroxide, *Langmuir*, 25 (2009) 10704-10710.
- [16] C. Forano, F. Bruna, C. Mousty, V. Prévot, Interactions Between Biological Cells and Layered Double Hydroxides: Towards Functional Materials, *Chem. Record*, 18 (2018) 1-18.

- [17] C. Mousty, O. Kaftan, V. Prevot, C. Forano, Alkaline phosphatase biosensors based on layered double hydroxides matrices: Role of LDH composition, *Sens. Actuators, B*, 133 (2008) 442-448.
- [18] M.B. Abdul Rahman, U.H. Zaidan, M. Basri, M.Z. Hussein, R.N.Z.R.A. Rahman, A.B. Salleh, Enzymatic synthesis of methyl adipate ester using lipase from *Candida rugosa* immobilised on Mg, Zn and Ni of layered double hydroxides (LDHs), *J. Mol. Catal. B: Enzymatic*, 50 (2008) 33-39.
- [19] F. Bruna, M.G. Pereira, M.L.T.M. Polizeli, J.B. Valim, Starch Biocatalyst Based on α -Amylase-Mg/Al-Layered Double Hydroxide Nanohybrids, *ACS Applied Materials & Interfaces*, 7 (2015) 18832-18842.
- [20] N. Touisni, F. Charmantray, V. Helaine, C. Forano, L. Hecquet, C. Mousty, Optimized immobilization of transketolase from *E. coli* in MgAl-layered double hydroxides, *Colloids Surf., B*, 112 (2013) 452-459.
- [21] C. Mousty, V. Prevot, Hybrid and biohybrid layered double hydroxides for electrochemical analysis, *Analytical and Bioanalytical Chemistry*, 405 (2013) 3513-3523.
- [22] R. Mahdi, C. Guérard-Hélaine, C. Laroche, P. Michaud, V. Prévot, C. Forano, M. Lemaire, Polysaccharide-layered double hydroxide-aldolase biohybrid beads for biocatalysed CC bond formation, *J. Mol. Catal. B: Enzymatic*, 122 (2015) 204-211.
- [23] M.D. Roldán, E. Pérez-Reinado, F. Castillo, C. Moreno-Vivián, Reduction of Polynitroaromatic Compounds: The Bacterial Nitroreductases, *FEMS Microbiol. Rev.*, 32 (2008) 474-500.
- [24] F.J. Peterson, R.P. Mason, J. Hovsepian, J.L. Holtzman, Oxygen-Sensitive and -Insensitive Nitroreduction by *Escherichia Coli* and Rat Hepatic Microsomes, *J. Biol. Chem.*, 254 (1979) 4009-4014.
- [25] D.W. Bryant, D.R. McCalla, M. Leeksa, P. Laneuville, Type I nitroreductases of *Escherichia coli*, *Can. J. Microbiol.*, 27 (1981) 81-86.
- [26] L. Carles, P. Besse-Hoggan, M. Joly, A. Vigouroux, S. Moréra, I. Batisson, Functional and structural characterization of two *Bacillus megaterium* nitroreductases biotransforming the herbicide mesotrione, *Biochem. J.*, 473 (2016) 1443-1453.
- [27] E. Dumas, M. Giraudó, E. Goujon, M. Halma, E. Khili, M. Stauffert, I. Batisson, P. Besse-Hoggan, J. Bohatier, P. Bouchard, H. Celle-Jeanton, M. Costa Gomes, F. Delbac, C. Forano, P. Goupil, N. Guix, P. Husson, G. Ledoigt, C. Mallet, C. Mousty, V. Prévot, C. Richard, S. Sarraute, Fate and ecotoxicological impact of new generation herbicides from the triketone family: An overview to assess the environmental risks, *J. Hazard. Mater.*, 325 (2017) 136-156.
- [28] S. Zenno, T. Kabori, M. Tanokura, K. Saigo, Conversion of NfsA, the Major *Escherichia coli* Nitroreductase, to a Flavin Reductase with an Activity Similar to That of Frp, a Flavin Reductase in *Vibrio harveyi*, by a Single Amino Acid Substitution, *J. Bacteriol.*, 180 (1998) 422-425.
- [29] Z. Naal, J.H. Park, S. Bernhard, J.P. Shapleigh, C.A. Batt, H.D. Abruna, Amperometric TNT Biosensor Based on the Oriented Immobilization of a Nitroreductase Maltose Binding Protein Fusion, *Anal. Chem.*, 74 (2002) 140-148.
- [30] N.V. Komarova, M.S. Andrianova, O.V. Gubanova, E.V. Kuznetsov, A.E. Kuznetsov, Development of a novel enzymatic biosensor based on an ion-selective field effect transistor for the detection of explosives, *Sensors and Actuators, B: Chemical*, 221 (2015) 1017-1026.
- [31] C. Berne, L. Betancor, H.R. Luckarift, J.C. Spain, Application of a Microfluidic Reactor for Screening Cancer Prodrug Activation Using Silica-Immobilized Nitrobenzene Nitroreductase, *Biomacromolecules*, 7 (2006) 2631-2636.

- [32] V.V. Gwenin, C.D. Gwenin, M. Kalaji, Colloidal Gold Modified with a Genetically Engineered Nitroreductase: Toward a Novel Enzyme Delivery System for Cancer Prodrug Therapy, *Langmuir*, 27 (2011) 14300-14307.
- [33] U.K. Laemmli, Cleavage of Structural Proteins during the Assembly of the Head of Bacteriophage T4., *Nature*, 227 (1970) 680-685.
- [34] M.M. Bradford, A rapid and sensitive method for the quantitation of microgram quantities of protein utilizing the principle of protein-dye binding, *Anal. Biochem.*, 72 (1976) 248-254.
- [35] C. Forano, U. Costantino, V. Prévot, C. Taviot-Gueho, Chapter 14.1 - Layered Double Hydroxides (LDH), in: F. Bergaya, G. Lagaly (Eds.) *Developments in Clay Science*, Elsevier 2013, pp. 745-782.
- [36] Z.P. Xu, G. Stevenson, C.-Q. Lu, G.Q. Lu, Dispersion and Size Control of Layered Double Hydroxide Nanoparticles in Aqueous Solutions, *J. Phys. Chem. B*, 110 (2006) 16923-16929.
- [37] C. Veschambres, M. Halma, E. Bourgeat-Lami, L. Chazeau, F. Dalmas, V. Prevot, Layered double hydroxides: Efficient fillers for waterborne nanocomposite films, *Appl. Clay Sci.*, 130 (2016) 55-61.
- [38] K. Benaissi, V. Helaine, V. Prevot, C. Forano, L. Hecquet, Efficient Immobilization of Yeast Transketolase on Layered Double Hydroxides and Application for Ketose Synthesis, *Advanced Synthesis & Catalysis*, 353 (2011) 1497-1509.
- [39] V. Prevot, C. Mousty, C. Forano, State of the art in biomolecule and layered double hydroxide assemblies, *Adv. Chem. Res.*, Nova Science Publishers, Inc. 2013, pp. 35-83.
- [40] N. Schultz, G. Metreveli, M. Franzreb, F.H. Frimmel, C. Syldatk, Zeta potential measurement as a diagnostic tool in enzyme immobilisation, *Colloids and Surfaces, B: Biointerfaces*, 66 (2008) 39-44.
- [41] E. Gasteiger, C. Hoogland, A. Gattiker, S. Duvaud, M.R. Wilkins, R.D. Appel, A. Bairoch, Protein Identification and Analysis Tools on the ExPASy Server., *The Proteomics Protocols Handbook*, Humana Press, Totowa, NJ, 2005, pp. 571-607.
- [42] B. Bjellqvist, G. Hughes, J., C. Pasquali, N. Paquet, F. Ravier, J.C. Sanchez, S. Frutiger, D. Hochstrasser, The focusing positions of polypeptides in immobilized pH gradients can be predicted from their amino acid sequences, *Electrophoresis*, 14 (1993) 1023-1031.
- [43] S. Vial, V. Prevot, F. Leroux, C. Forano, Immobilization of urease in ZnAl Layered Double Hydroxides by soft chemistry routes, *Micropor. Mesopor. Mater.*, 107 (2008) 190-201.
- [44] E. Geraud, V. Prevot, C. Forano, C. Mousty, Spongy gel-like layered double hydroxide-alkaline phosphatase nanohybrid as a biosensing material, *Chem. Commun.*, (2008) 1554-1556.
- [45] K. Charradi, C. Forano, V. Prevot, D. Madern, A. Ben Haj Amara, C. Mousty, Characterization of Hemoglobin Immobilized in MgAl-Layered Double Hydroxides by the Coprecipitation Method, *Langmuir*, 26 (2010) 9997-10004.
- [46] W. Kagunya, Z. Hassan, W. Jones, Catalytic Properties of Layered Double Hydroxides and Their Calcined Derivatives, *Inorg. Chem.*, 35 (1996) 5970-5974.
- [47] S.T. Frey, S.L. Guilmet, R.G. Egan III, A. Bennett, S.R. Soltau, R.C. Holz, Immobilization of the Aminopeptidase from *Aeromonas proteolytica* on Mg²⁺/Al³⁺ Layered Double Hydroxide Particles, *ACS Applied Materials & Interfaces*, 2 (2010) 2828-2832.
- [48] P. Satzer, F. Svec, G. Sekot, A. Jungbauer, Protein adsorption onto nanoparticles induces conformational changes: Particle size dependency, kinetics, and mechanisms, *Engineering in Life Sciences*, 16 (2016) 238-246.
- [49] W. Norde, My voyage of discovery to proteins in flatland ...and beyond, *Colloids and Surfaces, B: Biointerfaces*, 61 (2008) 1-9.
- [50] C.H. Giles, T.H. MacEwan, S.N. Nakhwa, D. Smith, 786. Studies in adsorption. Part XI. A system of classification of solution adsorption isotherms, and its use in diagnosis of adsorption

mechanisms and in measurement of specific surface areas of solids, *Journal of the Chemical Society (Resumed)*, (1960) 3973-3993.

[51] M. Rabe, D. Verdes, S. Seeger, Understanding protein adsorption phenomena at solid surfaces, *Adv. Colloid Interface Sci.*, 162 (2011) 87-106.

[52] R. Rojas, C.E. Giacomelli, Size-tunable LDH-protein hybrids toward the optimization of drug nanocarriers, *Journal of Materials Chemistry B*, 3 (2015) 2778-2785.

[53] J.R. Lakowicz, *Principles of Fluorescence Spectroscopy*, 3rd ed., Springer US2006.

[54] C. Duy, J. Fitter, How Aggregation and Conformational Scrambling of Unfolded States Govern Fluorescence Emission Spectra, *Biophys. J.*, 90 (2006) 3704-3711.

[55] F. Bellezza, A. Cipiciani, L. Latterini, T. Posati, P. Sassi, Structure and Catalytic Behavior of Myoglobin Adsorbed onto Nanosized Hydrotalcites, *Langmuir*, 25 (2009) 10918-10924.

[56] E. Herrera, J. Valdez Taubas, C.E. Giacomelli, d-Amino acid oxidase bio-functionalized platforms: Toward an enhanced enzymatic bio-activity, *Appl. Surf. Sci.*, 356 (2015) 679-686.

[57] W. Norde, C. Giacomelli, E. , Conformational changes in proteins at interfaces: From solution to the interface, and back, *Macromolecular Symposia*, 145 (1999) 125-136.

[58] F. Secundo, Conformational changes of enzymes upon immobilisation, *Chem. Soc. Rev.*, 42 (2013) 6250-6261.

[59] J. Kanga Wagheu, C. Forano, P. Besse-Hoggan, I.K. Tonle, E. Ngameni, C. Mousty, Electrochemical determination of mesotrione at organoclay modified glassy carbon electrodes, *Talanta*, 103 (2013) 337-343.

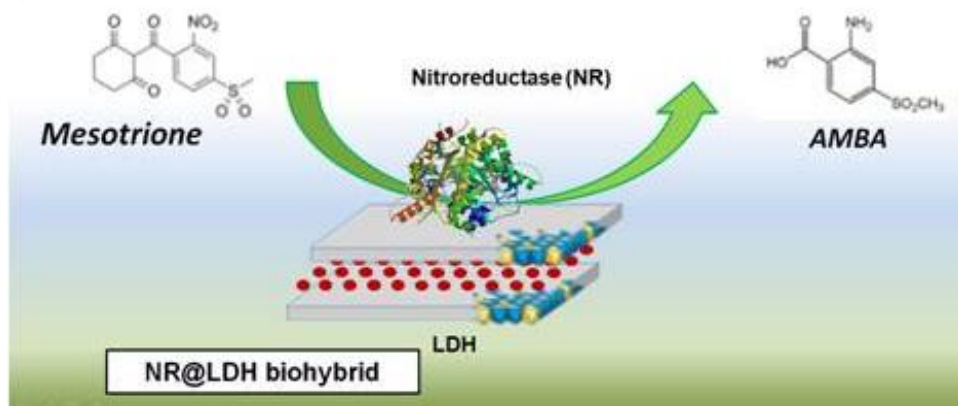
[60] A. Radoi, D. Compagnone, Recent advances in NADH electrochemical sensing design, *Bioelectrochem.*, 76 (2009) 126-134.

[61] S. Zenno, T. Kobori, M. Tanokura, K. Saigo, Purification and Characterization of NfrA1, a *Bacillus subtilis* Nitro/flavin Reductase Capable of Interacting with the Bacterial Luciferase, *Biosci., Biotechnol., Biochem.*, 62 (1998) 1978-1987.

[62] J.S. Caygill, S.D. Collyer, J.L. Holmes, F. Davis, S.P.J. Higson, Disposable screen-printed sensors for the electrochemical detection of TNT and DNT, *Analyst*, 138 (2013) 346-352.

[63] C. Taviot-Guého, V. Prévot, C. Forano, G. Renaudin, C. Mousty, F. Leroux, Tailoring Hybrid Layered Double Hydroxides for the Development of Innovative Applications, *Adv. Funct. Mater.*, 28 (2018) 1703868.

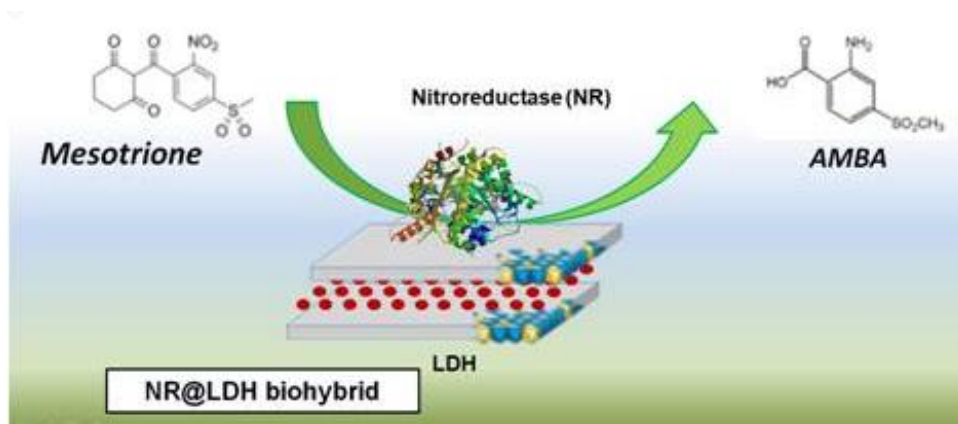
Table of Contents Graphic



Nitroreductase@Layered Double Hydroxide biohybrids were successfully prepared and tested toward the mesotrione biotransformation and detection.

ACCEPTED MANUSCRIPT

Table of Contents Graphic



Nitroreductase@Layered Double Hydroxide biohybrids were successfully prepared and tested toward the mesotrione biotransformation and detection.